
Déjà Vu Memorization in Vision-Language Models

Bargav Jayaraman¹ Chuan Guo¹ Kamalika Chaudhuri^{1 2}

Abstract

Vision-Language Models (VLMs) have emerged as the state-of-the-art representation learning solution, with myriads of downstream applications such as image classification, retrieval and generation. A natural question is whether these models memorize their training data, which also has implications for generalization. We propose a new method for measuring memorization in VLMs, which we call *déjà vu memorization*. For VLMs trained on image-caption pairs, we show that the model indeed retains information about individual objects in the training images beyond what can be inferred from correlations or the image caption. We evaluate *déjà vu* memorization at both sample and population level, and show that it is significant for OpenCLIP trained on as many as 50M image-caption pairs. Finally, we show that text randomization considerably mitigates memorization while only moderately impacting the model’s downstream task performance.

1. Introduction

Vision-Language Models (VLMs) have emerged as the state-of-the-art solution for learning representations from images and text data, with a number of downstream applications such as image generation (Ramesh et al., 2021; 2022; Yu et al., 2022), retrieval (Wang et al., 2015; Cao et al., 2016; Zhang et al., 2021; Baldrati et al., 2022), captioning (Mokady et al., 2021), and classification. At the same time, large foundation models are known to memorize and retain information about their training data (Carlini et al., 2019; Meehan et al., 2023; Carlini et al., 2023), and hence, a natural question is whether these Vision-Language Models *memorize* as well. If so, this raises questions about generalizability of these models. We investigate whether Vision-Language Models retain information about their training data beyond the bounds of generalization.

¹FAIR, Meta, California, USA ²University of California San Diego, California, USA. Correspondence to: Bargav Jayaraman <bargav@meta.com>.

The main challenge in measuring memorization is designing a measurement technique that can tease apart memorization from spurious correlations. For example, for an image of a black swan on water, a representation learning model may learn to predict *black swan* given the background *water* if either: (i) it retains extra information about the training image, or, (ii) if most of the examples in the training corpus with water also involve black swans. The first kind constitutes as memorization whereas the second kind is spurious correlation. This uncoupling of memorization from spurious correlation is particularly complicated for VLMs. Unlike generative models, VLMs as well as other representation learning models lack decoders that can directly generate images or text; therefore, what the model learns about its training data has to be detected more subtly. Prior work has looked into this problem for image-only representation models (Meehan et al., 2023) by measuring whether the model can predict the foreground of an image (e.g. black swan) beyond simple correlations based simply on its background (e.g. water). However, such simple solutions do not apply here. VLMs have two separate modalities – text and image, and the data sets used to train and evaluate them are considerably more complex than the simple foreground-background structure of ImageNet (see Figure 6 for an example). A consequence is that the image and text modalities can interact and transfer information in these models in subtly complex ways, making measurement significantly more challenging.

In this work, we propose a new method for measuring memorization in VLMs (depicted in Figure 1). Given a target image caption, we use the VLM to encode the caption and retrieve relevant image samples from a *public set* of images. Our test is based on the key insight that if an image-text pair is memorized by a VLM, then the retrieved images would resemble the training image to a significantly higher amount of detail than what is predictable from either the text caption or simple correlation. Formally, given a text-image pair, we retrieve an image from the model based on an embedding of its text description, and we measure what fraction of ground-truth objects in the original image also co-occur in the retrieved image. Then, to determine whether this happens simply due to correlation, we measure how this compares with the same statistic obtained from a similar VLM which does not have this image-text

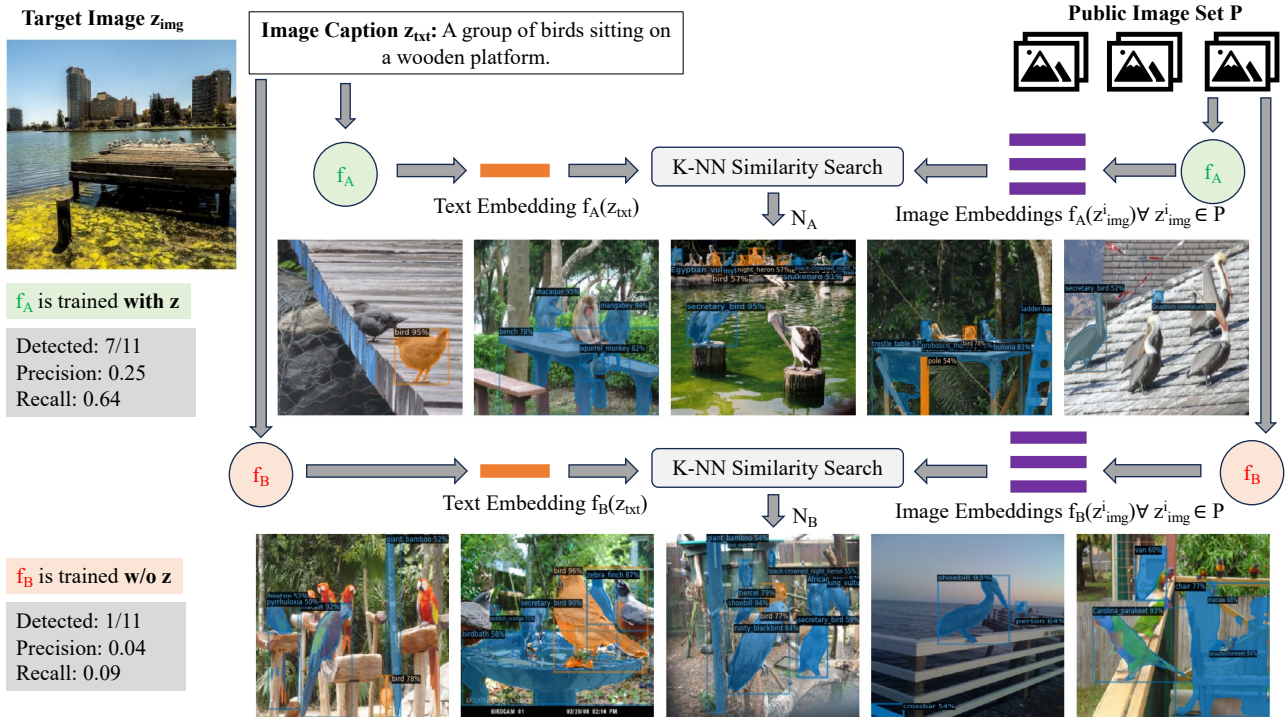


Figure 1: An example where an OpenCLIP model trained on a 50M subset of a filtered version of LAION and a subset of COCO exhibits *déjà vu memorization* of objects present in a training image. Public set is a collection of 1.28M images from ImageNet data set. The objects annotated in orange are true positives, i.e., the ones present in the target image, and the objects annotated in blue are false positives. For the OpenCLIP model f_A trained on the target image, our test recovers significantly more memorized objects compared to the model f_B that was not trained on the target image. Additional qualitative examples can be found in Figure 11 in the appendix.

pair in its training data. Combining these two steps gives us a measurement method that we call VL-Déjà-Vu.

We evaluate our test on OpenCLIP models trained on subsets of a filtered version of LAION with varying number of training samples. We find that even at training data set sizes where CLIP generalizes well, there is a significant degree of model memorization as depicted by our metrics (see Section 4). Finally, we explore mitigation measures that reduce information leakage in Section 5. We find that text masking significantly mitigates déjà vu memorization at a marginal cost to the model utility.

Contributions. Our main contributions are as follows.

- We propose VL-Déjà-Vu—a new way of measuring memorization in VLMs by measuring what fraction of ground-truth objects in an image can be predicted from its text description for a training image-text pair.
- Based on this measurement technique, we propose both (a) an individual sample-level test to detect memorization for individual text-image pairs and (b) an aggregate population-level test for a Vision-Language Model.

- We use our VL-Déjà-Vu test to evaluate memorization in OpenCLIP, and show that memorization does occur for VLMs trained using a number of different training set sizes and regularization parameter values, even for settings where the model generalizes well.
- Finally, we explore mitigation measures, and demonstrate that among a number of different ways of training OpenCLIP, random masking of text serves to significantly reduce déjà vu memorization.

2. Background

Vision-Language models are multi-modal models whose core function is to map image-text pairs into a pair of representations that are semantically relevant. These embeddings can then be used for downstream tasks such as image classification, captioning, retrieval and generation. VLMs are composed of a *vision block*, consisting of a convolutional network or a vision transformer, and a *text block*, consisting of a transformer, that produce image and text embeddings respectively from input image-text pairs. Given a trained vision-language model f , and an image-

text pair $z = \langle z_{img}, z_{txt} \rangle$, we denote the corresponding image and text embeddings as $f(z_{img})$ and $f(z_{txt})$. We consider VLMs that involve contrastive pre-training; in other words, during training, the model learns to minimize the distance between the image and text embeddings of the matching pairs in the training set D_{tr} while maximizing the distance of the mismatched pairs. The most commonly used contrastive loss is the InfoNCE loss (van den Oord et al., 2018) given as follows:

$$L = -\log \frac{\exp(f(z_{img}^i)^\top f(z_{txt}^i)/\tau)}{\sum_j \exp(f(z_{img}^i)^\top f(z_{txt}^j)/\tau)} \quad (1)$$

where τ is the temperature parameter and $z^j, \forall j \neq i$ are negative examples to contrast against. In practice, for each positive example z^i , we use all other examples in a training batch as negative examples.

The most popular VLM of this type is CLIP (Contrastive Language-Image Pre-Training; Radford et al. (2021)), trained on an undisclosed data set, which achieves competitive out-of-the-box performance across many transfer learning tasks. OpenCLIP (Ilharco et al., 2021) has released an open-source version of CLIP that is trained on the LAION data set ((Schuhmann et al., 2021)), and shows that it can achieve performance comparable with CLIP. Our work investigates memorization in OpenCLIP.

Memorization in ML models. It is well-known that machine learning models can memorize their training data in ways that enable data extraction. This phenomenon has been studied for both language (Carlini et al., 2019; 2021; Zanella-Béguelin et al., 2020; Jayaraman et al., 2022) and vision (Somepalli et al., 2023; Carlini et al., 2023; Sablayrolles et al., 2018; Meehan et al., 2023) models. However, all these works only consider the uni-modal setting, and as such the impact of this phenomenon is not clear in the multi-modal settings. Moreover, almost all the prior studies (except (Meehan et al., 2023)) focus on generative models – language or vision – where measuring memorization is easier because of the presence of a decoder. Similar to (Meehan et al., 2023), we consider the setting of representation learning models, where we do not have a decoder and instead only have access to an encoder. Although unlike (Meehan et al., 2023), who consider the vision models that capture the relationship between representation of the background of an image (such as water) and the label of its foreground object (such as black swan), we consider the settings where the models are trained on more complex data sets that have multiple objects in any given image. Such a simple foreground-background measurement does not directly apply to our setting of Vision Language Models where the two modalities may leak training data in more subtle and complicated ways. Our work builds upon

their test, and extends it to VLMs. A more detailed background discussion can be found in Appendix A.

3. Déjà Vu Memorization

Déjà vu memorization happens when a foundation model retains information about individual training data points beyond what is expected by simple correlation, and allows the recovery of such information during inference time. An example is when an image representation learning model can confidently predict the foreground of a training image based simply on its background (Meehan et al., 2023), while similar predictions cannot be made for test images.

In the context of Vision-Language Models, however, measuring déjà vu memorization is not as simple, due to the presence of multiple modalities as well as the complex nature of the training data. Compared to ImageNet, VLMs are trained on vastly more semantically rich data sets with many more objects as well as complicated captions, which may not capture everything in the image – see Figure 6 for an example. This means that the text and image modalities can interact and transfer information in subtly complex ways, making measurement significantly more challenging.

To resolve this challenge, we instead propose to measure whether the ground truth objects in an image can be predicted from the representation of its caption. We rely on the intuition that the caption of an image typically does not include all its objects, and hence high confidence recovery of this level of detail implies some form of memorization. If this prediction can be done significantly more accurately when the image is in the training set of a model than when it is in the test, then the image-text pair is being memorized by the said model.

Definition 1 (Déjà Vu Memorization) *A vision-language model f suffers from déjà vu memorization if it retains specific information about the individual training images that allows the recovery of objects present in the training images. In other words, for a target image-text pair $z = \langle z_{img}, z_{txt} \rangle$, more unique objects can be recovered from z_{img} given z_{txt} when z is present in f 's training set compared to when it is not.*

This is possible due to the model’s ability to encode the individual objects in the image embeddings, which is in turn reflected in the corresponding text embeddings when the model minimizes the contrastive loss during training. Next we will discuss how we quantify this phenomenon using two separate models (a target and a reference) as well as a nearest neighbor test.

Algorithm 1 k -Nearest Neighbor Test

Setup Phase

- 1: Sample two disjoint data sets A and B consisting of image–text pairs of the form $z = \langle z_{img}, z_{txt} \rangle$ and train models f_A and f_B on the respective data sets.
- 2: Sample a separate public set of images P that is disjoint from the images in A and B .
- 3: For each image $z_{img}^i \in P$, obtain the corresponding image embeddings from both the models, $f_A(z_{img}^i)$ and $f_B(z_{img}^i)$.

Testing Phase

- 4: Sample a record from A set, $z = \langle z_{img}, z_{txt} \rangle \in A$, and obtain the corresponding text embeddings from both the models, $f_A(z_{txt})$ and $f_B(z_{txt})$.
- 5: Obtain k public images $N_A \subseteq P$ and $N_B \subseteq P$ closest to z_{txt} in the embedding space for f_A and f_B respectively.
- 6: Evaluate the gap between the fraction of ground-truth objects detected in the sets N_A and N_B .

3.1. Measurement Methodology

Since VLMs are meant to capture general correlations between images and their text captions, our goal is to differentiate the recovery of ground-truth objects due to déjà vu memorization from spurious correlations alone. To enable this for a given image-text pair $z = \langle z_{img}, z_{txt} \rangle$, we use two separate VLMs f_A and f_B that are trained on randomly sampled but disjoint data sets A and B respectively. z lies in the training set of *exactly one* of these models, and hence by comparing the outputs of the two models, we can infer whether z was memorized. We do a k -nearest neighbor test using a separate public set of images as described in Algorithm 1 and find the subset of images that are closest to z in the representation space. The intuition here is to decode the objects present in these images.

3.2. Metrics

The k -nearest neighbor test in Algorithm 1 shows how to obtain predictions of the ground-truth objects given an image; we next use these predictions to develop population-level and sample-level memorization metrics. For our evaluation, we adopt the precision, recall and F-score metrics from the information retrieval literature to quantify the fraction of objects memorized by the models.

Sample-level metrics. At the sample level, we evaluate the fraction of ground-truth objects memorized by the target model from a given training image–text pair $z = \langle z_{img}, z_{txt} \rangle$. To do this, we run the nearest neighbor test on both the target and reference models, f_A and f_B , to obtain their respective neighbor sets N_A and N_B as per Algo-

rithm 1. We then calculate the *precision*, *recall* and *F-score* values when identifying the ground truth objects present in z_{img} using N_A and N_B and report the gap between the respective values for both the models. The precision, *prec*, and recall, *rec*, are given by the following equations:

$$\begin{aligned}
 rec(z, f_i) &= \frac{\# \text{ unique objects in } N_i \cap z_{img}}{\# \text{ unique objects in } z_{img}}; \forall i \in \{A, B\} \\
 prec(z, f_i) &= \frac{\# \text{ unique objects in } N_i \cap z_{img}}{\# \text{ unique objects in } N_i}; \forall i \in \{A, B\}
 \end{aligned}
 \tag{2}$$

F-score is the harmonic mean of precision and recall.

Population-level metrics measure what fraction of the training data is memorized by a model. For proper measurement, we propose three metrics: *population precision gap* (PPG), *population recall gap* (PRG) and *AUC gap* (AUCG). Given the notations defined in Algorithm 1, the population precision gap is the the fraction of data points from A where f_A has a higher precision in identifying the ground truth objects than f_B minus the fraction of data points where f_B has a higher precision in identifying the ground truth objects than f_A . Formally,

$$\begin{aligned}
 PPG &= \frac{1}{|A|} \left(|\{z \in A : prec(z, f_A) > prec(z, f_B)\}| \right. \\
 &\quad \left. - |\{z \in A : prec(z, f_A) < prec(z, f_B)\}| \right),
 \end{aligned}
 \tag{3}$$

where $|A|$ denotes the size of the set A and $prec(z, f_A)$ measures the precision of object prediction on z given the model f_A as defined in Equation 2. We define the population recall gap similarly:

$$\begin{aligned}
 PRG &= \frac{1}{|A|} \left(|\{z \in A : rec(z, f_A) > rec(z, f_B)\}| \right. \\
 &\quad \left. - |\{z \in A : rec(z, f_A) < rec(z, f_B)\}| \right),
 \end{aligned}
 \tag{4}$$

where $rec(z, f_A)$ measures the recall of object prediction on z given the model f_A as defined in Equation 2.

The PRG metric uses a binary test to check if the recall of f_A is greater than f_B on a given image, and obtains the aggregate value over the entire training set. We also visualize the fine-grained cumulative recall distribution of both the models over the training set as shown in Figure 7. This gives us a better understanding of what fraction of objects are recovered overall. We then measure the difference between the two distributions (i.e., for f_A and f_B) to simplify this information into a single quantity we call AUC gap.

While both the population-level and sample-level metrics rely on the precision and recall functions, they have subtle differences. First, population-level metrics measure the aggregate memorization over the entire training set whereas sample-level metrics measure the memorization in individual training samples. Second, population-level metrics rely

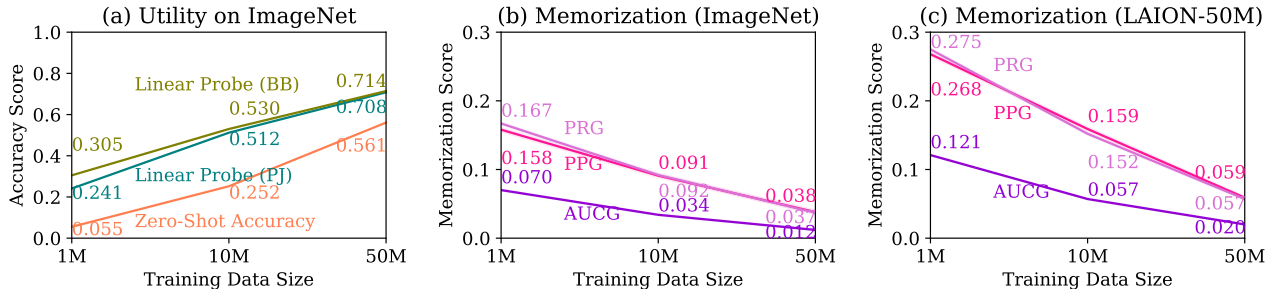


Figure 2: Performance of ViT-B-32 CLIP models with varying training data size sampled from filtered LAION. (a): model utility on ImageNet, where PJ refers to the 512-dimensional projector embedding and BB refers to the 768-dimensional backbone embedding. (b) and (c): population-level memorization of models with ImageNet and LAION-50M as public sets respectively, using the metrics defined in Section 3.2. For the memorization metrics, we report the *mean* \pm *std* values (*std* \leq 0.003) over 100 repetitions of randomly sampling 10% of records with replacement.

on binary tests to differentiate between the target and reference models and as such do not capture the magnitude of the gap between the models as is done by the sample-level metrics. We define both sets of metrics to capture the memorization at different granular levels and to be actionable in a meaningful way, thereby allowing the model developers to fine-tune the models to mitigate the memorization risk.

4. Evaluating Déjà Vu Memorization

We next apply the metrics designed in Section 3.1 to determine if CLIP memorizes training data. Specifically, we seek to answer the following two research questions:

1. How does déjà vu memorization of CLIP vary with training set size and number of training epochs?
2. Are all training data points memorized uniformly?

These questions are considered in the context of OpenCLIP trained on different subsets of a filtered version of LAION data set (Radenovic et al., 2023). We sample up to 50M image-text pairs from the data set and train OpenCLIP models with ViT-B-32 architecture. For the public set, we consider (a) another non-overlapping subset of 50M image-text pairs from filtered LAION (called LAION-50M) and (b) the entire ImageNet training set (Deng et al., 2009).

4.1. Model Utility

As mentioned above, we trained models with different training set sizes consisting of 1M/10M/50M image-text pairs. We use linear probe and zero-shot performance on ImageNet to evaluate the utility of these models. For the linear probe task, we take either the 768-dimensional backbone (BB) layer or the 512-dimensional projector (PJ) layer image embeddings of the model on each image and use it to

train a logistic regression probe model that predicts the object label of the image. The accuracy of this probe model on a test set is then considered as the linear probe accuracy. For zero-shot classification we use the same setup as in OpenCLIP. Figure 2 shows the model utility in terms of linear probe and zero-shot accuracy on ImageNet.

4.2. Measuring Population-Level Memorization

For quantifying population-level memorization, we measure the gap between the object recall distributions for the target and reference models. If there were no memorization, we would observe virtually no gap between the two distributions, i.e. AUCG = 0. Figure 7 shows the object recall distribution gap between the target and reference models for varying training set sizes when ImageNet is used as the public set. When the training set size is small (e.g. 1M as shown in the left-most figure), there is a higher déjà vu memorization due to the models overfitting on the training set. As the training set size increase from 1M up to 50M, the gap decreases confirming that the models begin to generalize better. Note that the memorization is still significant for models trained on 10M data set. We consider this setting for further experiments as this is a typical training set size for many foundation models in practice (Ilharco et al., 2021). For instance, it is common to train CLIP models on the 12M Conceptual Captions data set (Sharma et al., 2018) or the 15M subset of the YFCC data set (Thomee et al., 2016). We also tried measuring the AUC gap for the precision distributions but found it to be low even for highly overfitted models. Moreover, the precision AUC gap also seems to be less sensitive to parameter changes that we try later in Section 5. Thus we stick with the recall gap as it captures the risk we want to highlight (i.e. what fraction of the ground-truth objects are recovered).

Apart from the AUCG metric, we also quantify the gap in

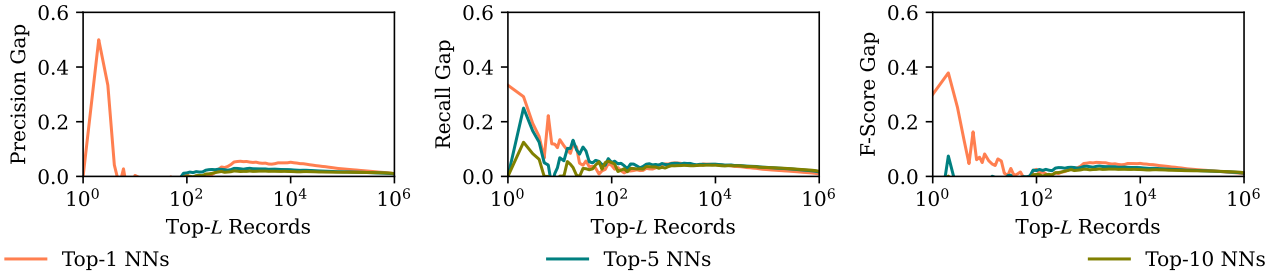


Figure 3: Sample-level memorization gap between target and reference models when predicting top-10 objects for different top- L records. Records are sorted w.r.t. the embedding distance. Models are trained on disjoint 10M subsets of filtered LAION data set for 200 epochs and ImageNet public set is used for the KNN test.

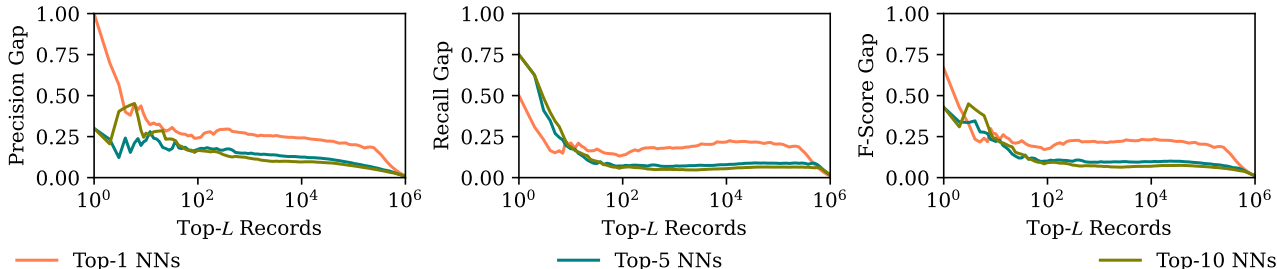


Figure 4: Sample-level memorization gap between target and reference models when predicting top-10 objects for different top- L records. Records are sorted w.r.t. the decreasing number of correct object predictions for target model. Models are trained on disjoint 10M subsets of filtered LAION data set for 200 epochs.

terms of the PPG and PRG metrics. Figure 2 shows the PPG, PRG and AUCG metric values for models trained with different training set sizes using both ImageNet and LAION-50M public sets. Recall that LAION-50M has no overlap with the model training sets. While the absolute metric values are higher for the LAION-50M public set compared to those for the setting where ImageNet is used as the public set, the trend remains the same: memorization decreases with increasing training set size as the models begin to generalize better. In Section 5, we explore various approaches to reduce this memorization.

4.3. Measuring Sample-Level Memorization

While the population-level metrics like AUCG, PPG and PRG show evidence of memorization, they do not pinpoint which training images are more vulnerable. We sort the training data in decreasing order of memorization to show the subset of most vulnerable records. To do this, we explore several sorting metrics. The most straightforward metric is the distance between the training text embedding and the nearest neighbour public image embeddings obtained using Algorithm 1. The records for which the public image embeddings are the closest are more easily memorized by the model. Compared to the population-level memorization, where we keep the experiments parameter-free to the best extent, at the sample-level we want to focus on more fine-grained leakage so we choose top-10 object

labels to measure the gap instead of predicting all the objects. Figure 3 shows the precision, recall and F-score gaps between the target and reference models for varying top- k records sorted with respect to this distance metric where ImageNet is used as the public set. As shown, the gaps can be greater than 0.3 for top-1 and top-10 records.

We also tried sorting the records in the decreasing order of the number of objects correctly identified using the target model with the nearest neighbor test. Figure 4 shows the precision, recall and F-score gaps for the records sorted using this metric. We see that the gap can become very significant for the top-1 and top-10 records. Although this metric requires the ground truth labels which the adversary would not have access to in practice, this is still useful to visualize the worst case examples. Results for sample-level memorization using the LAION-50M public set show a similar trend and can be found in Section C.1.

Key Observations. We show déjà vu memorization at both population and sample levels. At the population-level, where we measure the aggregate memorization of model over the training set, we find that the memorization decreases with an increase in the training set size. This could be attributed to improved model generalization. At the sample-level, we note that the model memorizes disproportionately—a subset of training image-text pairs are memorized more than the others.

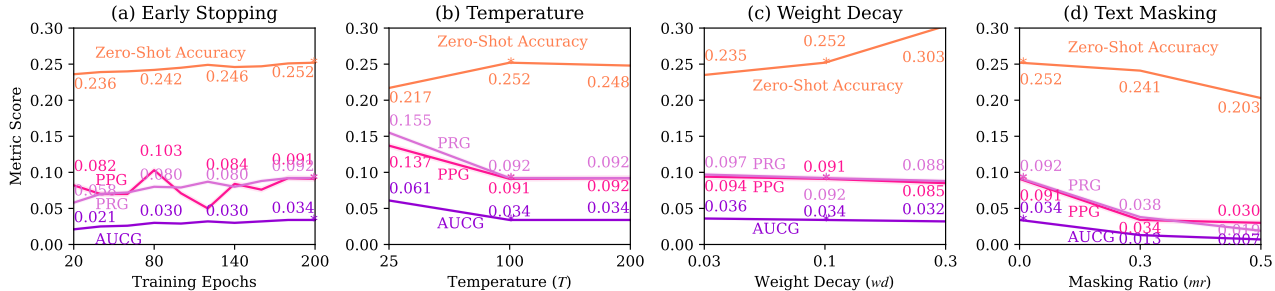


Figure 5: Effect of mitigation on ViT-B-32 OpenCLIP models trained on 10M subset of filtered LAION. Memorization evaluation is done using ImageNet as public set. Default setting is highlighted with asterisk. For the memorization metrics, we report the *mean ± std* values (*std* ≤ 0.003) over 100 repetitions of randomly sampling 10% of records with replacement.

5. Mitigation

How can we mitigate déjà vu memorization in VLMs? Since it presumably happens due to the model overfitting on training data, it is likely that regularization techniques may be able to mitigate it. We investigate the impact of four regularization techniques on déjà vu memorization.

1. *Early stopping* is a common technique for regularizing neural networks where model training is ended prematurely. It is effective due to the observation that models begin to overfit on the training set when they are trained for more epochs.
2. *Temperature* is the contrastive loss parameter that controls how close the text and image embeddings can get during the model training. Changing the temperature parameter has a regularization effect for SSL as observed by Meehan et al. (2023).
3. *Weight decay*, also known as L_2 regularization, is a standard regularization technique for ML models.
4. To reduce overfitting along the text and image modalities in VLMs, we look at additional regularization through *text randomization*, where we randomly mask a fraction of the text tokens during training. We parameterize the amount of randomization through *masking ratio*, which measures the fraction of text tokens masked.

In the following we present results when ImageNet is used as the public set for the nearest neighbor test. Results for the LAION-50M public set can be found in Section C.2.

5.1. Early Stopping

It is widely believed that deep learning models begin to overfit on the training data as the number of training epochs increases. It is thus a good practice to early stop the training as soon as the model utility on a hold-out test set stagnates or begins to drop. However this is often not the case for SSL models. It is not uncommon to observe that the zero-shot accuracy of SSL models keeps improving as the mod-

els are trained for longer (Meehan et al., 2023). Regardless, we still explore early stopping as a mitigation mechanism. As shown in Figure 5, training the CLIP model for more epochs leads to better zero-shot accuracy, but at the same time, déjà memorization also increases. This is in line with our hypothesis above. Even when we early stop the model at 20 epochs (10% of the default parameter value of 200 epochs), the memorization risk is not completely mitigated although the absolute values are lower.

5.2. Temperature Scaling

Temperature, or logit scale, controls how close the text and image embeddings can get during training. Smaller values allow for the multi-modal embeddings to get closer, and as a consequence the CLIP contrastive loss drops quickly, whereas larger values regularize the loss but may lead to training instability as noted by Radford et al. (2021). The default value in OpenCLIP implementation is set to 100. We vary this value between 25, 100 and 200. As shown in Figure 5, decreasing the temperature (T) from 100 to 25 decreases the model’s zero-shot classification accuracy on ImageNet from 25.2% to 21.7% and also increases the memorization as indicated by the increase in the PPG, PRG and AUCG metrics. This is due to the decrease in the distance between the text and image embeddings for the training data which could potentially lead to model overfitting. Increasing the temperature to 200 moderately impacts the model’s zero-shot classification accuracy and the memorization leakage remains more or less the same.

5.3. Weight Decay

Weight decay directly controls the model overfitting, with larger values corresponding to stronger regularization. The default value is set to 0.1 and we vary it between 0.03, 0.1 and 0.3. As expected, decreasing the weight decay wd from 0.1 to 0.03 decreases the model’s zero-shot classification accuracy and also worsens the leakage due to memorization

as shown in Figure 5. Interestingly, increasing the weight decay to 0.3 significantly improves the model’s zero-shot accuracy. We believe that the default value of 0.1 is not optimal for the 10M training set size as it was set based on the model training for larger data sizes (possibly on the entire LAION data set). With 0.3 weight decay, we observe a consistent decrease in the population memorization leakage, as shown by the PPG, PRG and AUCG values for $wd = 0.3$ in Figure 5, but the values are still significantly high. We also explored setting weight decay to 0.01 and 1.0, but they either adversely impacted the model utility or severely increased memorization. Thus while tuning wd does not completely mitigate memorization, we can get a reasonable trade-off in the neighbourhood of $wd = 0.3$.

5.4. Text Randomization

During model training, the CLIP models increase the cosine similarity between the matching image-caption pairs while simultaneously decreasing the cosine similarity between mismatching pairs to reduce the contrastive loss. While it is common to augment the training images to reduce overfitting, the text captions are not randomized. This could lead to the model overfitting on the text captions when minimizing the contrastive loss. To avoid this, we propose text randomization as a defense. For COCO subset of the training set, we randomly choose one out of the five captions for each image per epoch during training. For filtered LAION subset of the training set, we randomly mask a fraction of caption tokens since only a single caption is available per image in the filtered LAION data set. We vary the masking ratio between 0 (no masking), 0.3 and 0.5 (randomly mask half of the tokens).

We find this defense to work the best in mitigating déjà vu memorization but at the cost of model utility. As shown in Figure 5, using a masking ratio of 0.3 reduces the ImageNet zero-shot accuracy from 25.2% (in the default case when $mr = 0.0$) to 24.1%, but at the same time this significantly reduces the memorization leakage. The PPG metric reduces from 9.1% to 3.4%, and the PRG metric reduces from 9.2% to 3.8%. Moreover, the recall CDF gap (AUCG) also reduces from 0.034 to 0.013. Further increasing the masking ratio to 0.5 mitigates the risk even more. PPG reduces to 3.0%, PRG reduces to 1.9%, and AUCG reduces to only 0.007. We would expect a significant drop in the model utility if we increase mr beyond this value since the captions would have considerably less information.

Key Observations. We study the impact of tuning four regularization parameters: number of training epochs, temperature, weight decay and masking ratio. We find that early stopping reduces memorization but at the cost of model utility. Increasing the temperature increases the model zero-shot accuracy and decreases memorization up

to a certain threshold, beyond which the model utility begins to decrease. Surprisingly, we find that the default value of 100 already gives the optimal results. Similar to temperature, increasing the weight decay increases the model utility and decreases the memorization up to a certain threshold. We find 0.3 weight decay to achieve the best results for a model trained over 10M data. We observe a sharp decrease in model utility beyond this value. Text masking seems to be most effective in mitigating memorization. Increasing the masking ratio decreases memorization and also decreases the model utility. Masking ratio of 0.3 achieves a good trade-off by significantly reducing memorization while only moderately impacting the model utility.

6. Discussion

Prior works have mainly shown memorization in the unimodal setting: either for the language models (Carlini et al., 2019) or for vision models (Meehan et al., 2023). We have demonstrated that even in the complex multi-modal setting, ML models suffer from memorization. Moreover, while prior works have only evaluated memorization for small training data sizes (typically on the scale of 1 million or less), we show memorization on a wide scale, from 1 million to 50 million training set size. Our experiments show that while the population-level memorization metrics decrease with increase in the training set size, there remain strongly memorized examples as exemplified by the sample-level memorization where the model disproportionately memorizes a subset of records. Careful tuning of right hyper-parameters can, however, mitigate this memorization risk. We propose a suite of metrics to quantify déjà vu memorization in hope of guiding ML practitioners to train models in a safe way. These metrics not only quantify the risk in a meaningful and interpretable manner, but are also sensitive to the tuning of the mitigation parameters, thereby aiding the practitioners in choosing the right model hyper-parameter values that achieve a good utility-risk trade-off.

Broader Impact

We demonstrate that multi-modal models can memorize the objects present in the training images. While our intent is to make this risk more transparent to aid researchers get a deeper understanding of the memorization issue inherent in representation learning models, an adversary could potentially use this to launch attacks on CLIP-style models. Although such an adversary would need non-trivial amount of background information for a successful attack. For instance, the adversary would need at least access to two models such that exactly one of the two is trained on a target image-text pair. They would also need access to the underlying training data for the target model. We discuss the approaches that are effective at mitigating this risk.

References

- Alberto Baldrati, Marco Bertini, Tiberio Uricchio, and Alberto Del Bimbo. Conditioned and Composed Image Retrieval Combining and Partially Fine-Tuning CLIP-Based Features. In *Proceedings of the IEEE/CVF Conference on Computer Vision and Pattern Recognition (CVPR) Workshops*, 2022.
- Yue Cao, Mingsheng Long, Jianmin Wang, Qiang Yang, and Philip S Yu. Deep Visual-Semantic Hashing for Cross-Modal Retrieval. In *Proceedings of the 22nd ACM SIGKDD International Conference on Knowledge Discovery and Data Mining*, 2016.
- Nicholas Carlini, Chang Liu, Úlfar Erlingsson, Jernej Kos, and Dawn Song. The Secret Sharer: Evaluating and Testing Unintended Memorization in Neural Networks. In *28th USENIX Security Symposium (USENIX Security 19)*, 2019.
- Nicholas Carlini, Florian Tramer, Eric Wallace, Matthew Jagielski, Ariel Herbert-Voss, Katherine Lee, Adam Roberts, Tom Brown, Dawn Song, Úlfar Erlingsson, et al. Extracting Training Data from Large Language Models. In *30th USENIX Security Symposium (USENIX Security 21)*, 2021.
- Nicolas Carlini, Jamie Hayes, Milad Nasr, Matthew Jagielski, Vikash Sehwal, Florian Tramer, Borja Balle, Daphne Ippolito, and Eric Wallace. Extracting Training Data from Diffusion Models. In *32nd USENIX Security Symposium (USENIX Security 23)*, 2023.
- Jia Deng, Wei Dong, Richard Socher, Li-Jia Li, Kai Li, and Li Fei-Fei. ImageNet: A large-scale hierarchical image database. In *2009 IEEE conference on computer vision and pattern recognition*. IEEE, 2009.
- Rachna Dhamija and Adrian Perrig. Déjà Vu—A User Study: Using Images for Authentication. In *9th USENIX Security Symposium (USENIX Security 00)*, 2000.
- Matt Fredrikson, Somesh Jha, and Thomas Ristenpart. Model Inversion Attacks that Exploit Confidence Information and Basic Countermeasures. In *Proceedings of the 22nd ACM SIGSAC Conference on Computer and Communications Security*, 2015.
- Gabriel Ilharco, Mitchell Wortsman, Ross Wightman, Cade Gordon, Nicholas Carlini, Rohan Taori, Achal Dave, Vaishaal Shankar, Hongseok Namkoong, John Miller, Hannaneh Hajishirzi, Ali Farhadi, and Ludwig Schmidt. OpenCLIP, 2021. URL <https://doi.org/10.5281/zenodo.5143773>.
- Bargav Jayaraman and David Evans. Are Attribute Inference Attacks Just Imputation? *arXiv:2209.01292*, 2022.
- Bargav Jayaraman, Esha Ghosh, Melissa Chase, Sambudha Roy, Wei Dai, and David Evans. Combing for Credentials: Active Pattern Extraction from Smart Reply. *arXiv:2207.10802*, 2022.
- Diederik P. Kingma and Jimmy Ba. Adam: A Method for Stochastic Optimization. *arXiv:1412.6980*, 2017.
- Tsung-Yi Lin, Michael Maire, Serge Belongie, James Hays, Pietro Perona, Deva Ramanan, Piotr Dollár, and C Lawrence Zitnick. Microsoft COCO: Common Objects in Context. In *Computer Vision—ECCV 2014: 13th European Conference, Zurich, Switzerland, September 6–12, 2014, Proceedings, Part V 13*. Springer, 2014.
- Casey Meehan, Florian Bordes, Pascal Vincent, Kamalika Chaudhuri, and Chuan Guo. Do SSL Models Have Déjà Vu? A Case of Unintended Memorization in Self-supervised Learning. *arXiv:2304.13850*, 2023.
- Ron Mokady, Amir Hertz, and Amit H Bermano. ClipCap: CLIP Prefix for Image Captioning. *arXiv:2111.09734*, 2021.
- Filip Radenovic, Abhimanyu Dubey, Abhishek Kadian, Todor Mihaylov, Simon Vandenhende, Yash Patel, Yi Wen, Vignesh Ramanathan, and Dhruv Mahajan. Filtering, Distillation, and Hard Negatives for Vision-Language Pre-Training. In *Proceedings of the IEEE/CVF Conference on Computer Vision and Pattern Recognition*, 2023.
- Alec Radford, Jong Wook Kim, Chris Hallacy, Aditya Ramesh, Gabriel Goh, Sandhini Agarwal, Girish Sastry, Amanda Askell, Pamela Mishkin, Jack Clark, Gretchen Krueger, and Ilya Sutskever. Learning Transferable Visual Models from Natural Language Supervision. In *International conference on machine learning*. PMLR, 2021.
- Aditya Ramesh, Mikhail Pavlov, Gabriel Goh, Scott Gray, Chelsea Voss, Alec Radford, Mark Chen, and Ilya Sutskever. Zero-Shot Text-to-Image Generation. In *International Conference on Machine Learning*. PMLR, 2021.
- Aditya Ramesh, Prafulla Dhariwal, Alex Nichol, Casey Chu, and Mark Chen. Hierarchical Text-Conditional Image Generation with CLIP Latents. *arXiv:2204.06125*, 2022.
- Alexandre Sablayrolles, Matthijs Douze, Cordelia Schmid, and Hervé Jégou. Déjà Vu: an empirical evaluation of the memorization properties of ConvNets. *arXiv:1809.06396*, 2018.

- Christoph Schuhmann, Richard Vencu, Romain, Robert Kaczmarczyk, Clayton Mullis, Aarush Katta, Theo Coombes, Jenia Jitsev, and Aran Komatsuzaki. LAION-400M: Open Dataset of CLIP-Filtered 400 Million Image-Text Pairs. *arXiv:2111.02114*, 2021.
- Piyush Sharma, Nan Ding, Sebastian Goodman, and Radu Soricut. Conceptual Captions: A Cleaned, Hypernymed, Image Alt-text Dataset For Automatic Image Captioning. In *Proceedings of the 56th Annual Meeting of the Association for Computational Linguistics (Volume 1: Long Papers)*. Association for Computational Linguistics, 2018. URL <https://aclanthology.org/P18-1238>.
- Reza Shokri, Marco Stronati, Congzheng Song, and Vitaly Shmatikov. Membership Inference Attacks Against Machine Learning Models. In *2017 IEEE Symposium on Security and Privacy (SP)*. IEEE, 2017.
- Gowthami Somepalli, Vasu Singla, Micah Goldblum, Jonas Geiping, and Tom Goldstein. Diffusion art or digital forgery? investigating data replication in diffusion models. In *Proceedings of the IEEE/CVF Conference on Computer Vision and Pattern Recognition*, pages 6048–6058, 2023.
- Bart Thomee, David A. Shamma, Gerald Friedland, Benjamin Elizalde, Karl Ni, Douglas Poland, Damian Borth, and Li-Jia Li. YFCC100M: The New Data in Multimedia Research. *Commun. ACM*, 2016. doi: 10.1145/2812802. URL <https://doi.org/10.1145/2812802>.
- Aaron van den Oord, Yazhe Li, and Oriol Vinyals. Representation Learning with Contrastive Predictive Coding. *arXiv:1807.03748*, 2018.
- Daixin Wang, Peng Cui, Mingdong Ou, and Wenwu Zhu. Deep Multimodal Hashing with Orthogonal Regularization. In *Twenty-fourth international joint conference on artificial intelligence*, 2015.
- Samuel Yeom, Irene Giacomelli, Matt Fredrikson, and Somesh Jha. Privacy Risk in Machine Learning: Analyzing the Connection to Overfitting. In *2018 IEEE 31st Computer Security Foundations Symposium (CSF)*. IEEE, 2018.
- Jiahui Yu, Yuanzhong Xu, Jing Yu Koh, Thang Luong, Gunjan Baid, Zirui Wang, Vijay Vasudevan, Alexander Ku, Yinfei Yang, Burcu Karagol Ayan, et al. Scaling Autoregressive Models for Content-Rich Text-to-Image Generation. *arXiv:2206.10789*, 2022.
- Santiago Zanella-Béguelin, Lukas Wutschitz, Shruti Tople, Victor Rühle, Andrew Paverd, Olga Ohrimenko, Boris Köpf, and Marc Brockschmidt. Analyzing Information Leakage of Updates to Natural Language Models. In *Proceedings of the 2020 ACM SIGSAC conference on computer and communications security*, 2020.
- Peng-Fei Zhang, Yang Li, Zi Huang, and Hongzhi Yin. Privacy Protection in Deep Multi-Modal Retrieval. In *Proceedings of the 44th International ACM SIGIR Conference on Research and Development in Information Retrieval*, 2021.
- Xingyi Zhou, Rohit Girdhar, Armand Joulin, Philipp Krähenbühl, and Ishan Misra. Detecting Twenty-thousand Classes using Image-level Supervision. In *ECCV*, 2022.

A. Background and Related Work

Foundation models, such as large language models, have been long known to memorize their training data in ways that enable easy extraction. For example, a line of work (Carlini et al., 2019; 2021; Zanella-Béguelin et al., 2020; Jayaraman et al., 2022) has shown that large language models exactly memorize sequences of text tokens from the training data, and these text tokens can be extracted. Somepalli et al. (2023); Carlini et al. (2023) showed that diffusion models can generate images that are semantically and stylistically similar to training images or even their near-exact copies under certain circumstances. However, almost all prior studies that demonstrate this kind of memorization focus on generative models – language or vision – where measuring memorization is easier because of the presence of a decoder. In contrast, our work is concerned with representation learning models, where we simply have an encoder.

Sablayrolles et al. (2018) study déjà vu¹ memorization in neural networks and show that it is possible to infer whether an image or a subset of images was used in model training. Our work is also closely related to Meehan et al. (2023), which measures déjà vu memorization in image representation models. They show that given the representation of the background of an image, (such as water), the label of its foreground object (such as black swan) can be predicted

¹We note that many prior works have used the term “déjà vu” in different contexts. Dhamija and Perrig (2000) use this to refer to the ability of humans to recognize images, and they use it as a proxy for password-based authentication. Sablayrolles et al. (2018) denote déjà vu to essentially mean membership inference, where they test if a model *remembers* if an image was used in training. Meehan et al. (2023) refer to déjà vu as the ability of inferring foreground objects from vision models given a background patch of pixels. We use this term to refer to a vision-language model’s ability to recall the individual objects in the training images.

reliably. Moreover, this prediction is significantly more accurate for images in the training set of a model, thus showing that the models memorize their training data beyond the bounds of spurious correlation. However, such a simple foreground-background measurement does not directly apply to the more complex, multi-modal Vision Language Models where the two modalities may leak training data in more subtle and complicated ways. Our work builds upon their test, and extends it to VLMs.

Finally, there has been a body of work on empirical measurement of privacy, and broadly speaking, there are three main kinds of attacks. In membership inference (Shokri et al., 2017), the goal is to determine if a specific data point was used to train a model. In attribute inference (Yeom et al., 2018), the goal is to infer unknown features or attributes of a data point based on a model trained on this or similar points. Finally, training data reconstruction attacks (Fredrikson et al., 2015) aim to recover one or more training data points given a model and some auxiliary information. Our work falls within the purview of attribute inference. However, unlike most attribute inference attacks which were shown to be forms of statistical imputation (Jayaraman and Evans, 2022), our tests directly measure how much more effective attribute inference can be when a data point is in the training set of a model.

B. Detailed Experiment Setup

For our experiments we use the OpenCLIP implementation (Ilharco et al., 2021), and train models over subsets of a filtered version of LAION (Radenovic et al., 2023) and MS-COCO (Lin et al., 2014) data sets. As discussed in Algorithm 1, our test requires disjoint training sets A and B to train the models f_A and f_B respectively. To obtain the two non-overlapping training sets, we sample 40K image-text pairs from COCO data set and 1M/10M/50M image-text pairs from filtered LAION data set to form A set, and repeat the process to obtain the B set.

We use the ViT-B-32 CLIP model architecture consisting of around 151M trainable parameters and train the models for 200 epochs using Adam (Kingma and Ba, 2017) optimizer with cosine learning rate scheduler and a learning rate of 0.0005. We use 256 commodity GPUs to train the models in parallel with an effective batch size of 16 384. All other hyper-parameters are set to the default value as used in OpenCLIP; we do an ablation study on the impact of temperature and weight decay in Section 5.

We take the 1.28M images from ImageNet data set (Deng et al., 2009) and perform face-blurring to form our public set P . We also consider a larger public set consisting of a separate subset of 50M images from filtered LAION that has no overlap with the A and B sets. We call this LAION-

50M and include most of the results on this public set in Appendix C. We use the metrics defined in Section 3.2 to quantify the déjà vu memorization in our experiments.

Obtaining Object Annotations. For quantitative evaluation of our nearest neighbor tests, we require detailed object annotations for the A , B and P sets. The filtered LAION data set only has image captions and no object annotations. ImageNet originally has only one object annotation per image, as shown in Figure 6. Hence, we use an open-source annotation tool, called Detic (Zhou et al., 2022), to obtain multiple fine-grained object annotations per image for all our data sets. This tool can annotate all the 21K ImageNet objects. Even though COCO has multiple object annotations, its class label space is small (i.e., only 80 unique classes). Hence we use Detic on COCO to extend its annotations and to make the label annotations consistent across all the data sets we use. Figure 1 shows the sample images with multiple object annotations obtained using Detic.

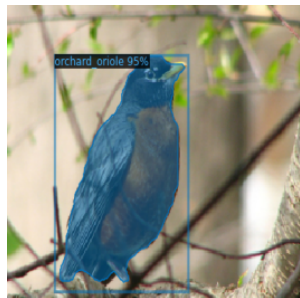
Limitations in Experimental Evaluation. We find that the object annotation tool, Detic (Zhou et al., 2022), is not always accurate. For instance, the tool often classifies a ‘polar bear’ as ‘jaguarundi’. However, our experiments rely on the relative gap in the object detection between the target and reference models and as such are robust to these inaccuracies as long as the annotations are consistent across the images. For instance, if the ‘polar bear’ is classified as ‘jaguarundi’ across all the public set images, the gap between the ‘polar bear’ detection accuracy of target and reference models, based on our nearest neighbor test, will remain consistent. While the absolute numbers in our quantitative tests may vary based on the object annotation tool used, our experimental observations would not change.

C. Additional Results with LAION-50M

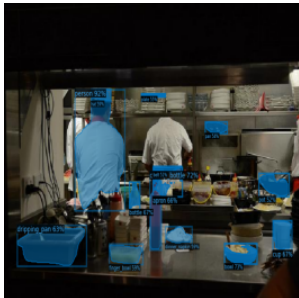
In Section 4, we discussed the memorization results considering the ImageNet as the public set for our nearest neighbor test. Here we discuss the results with a much larger LAION-50M data set as the public set. While the overall trend remains the same as with the ImageNet, with a richer public set, we are able to achieve a larger memorization gap for our models.

C.1. Sample-Level Memorization

Similar to the sample-level evaluation for ImageNet public set in Section 4.3, we evaluate the gap in precision, recall and F-scores of top- k records sorted with respect to the minimum embedding distance when considering LAION-50M as the public set for the nearest neighbor test. Figure 8 shows the memorization gap of the top- k records. We note a greater precision gap with top-1 nearest neighbor when



Label:
Orchard Oriole.



Caption:
Several kitchen workers making dishes in commercial kitchen.
Labels:
Catsup Bottle, Pot, Hat, Plate, Dinner Napkin, Finger Bowl, Soda Can, Bottle, Dripping Pan, Cup, Work Shirt, Bowl, Apron, Person, Belt, Pan.

(a) Sample Image from ImageNet.

(b) Sample Image from COCO.

Figure 6: Comparing images from ImageNet and COCO data sets. The ImageNet images only have single label per image but COCO images have complex scenes with multiple object labels. Additionally, COCO images have accompanying text captions. Label annotations with bounding boxes are highlighted in blue for both the images.

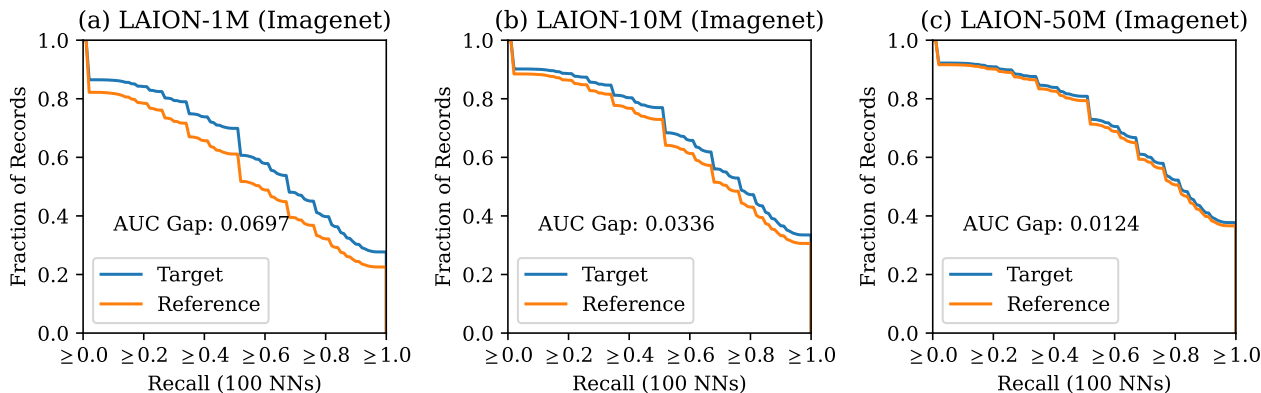


Figure 7: Object recall distribution of target and reference models trained for 200 epochs over different training sizes.

compared to the case where ImageNet was used as a public set (see Figure 3). However, the recall gap is lower with this public set. These variations could be due to the nature of the public set—many LAION images have few or no annotations. This does not mean that the sample-level memorization risk is lower. As shown in Figure 9, the memorization gap is much higher for this public set when we sort the records in the decreasing order of the number of correct predictions made by the target model using the nearest neighbor test. This corroborates our population-level memorization results in Figure 2 where we find a higher memorization gap with LAION-50M public set.

C.2. Mitigation

We observe similar trends for mitigation with different regularization parameters as with the ImageNet case. Figure 10 shows the impact of different parameters on the memorization. Since the LAION-50M public set is much larger than the ImageNet public set, the overall memoriza-

tion values are higher due to the public set nearest neighbors being more representative of the target image, and thus capturing more objects. However, the trend remains the same. Increasing the temperature decreases the memorization, but the default value of 100 is close to optimal as the trade-off between memorization and model utility is the best. Increasing the weight decay improves the model utility (indicated by the zero-shot accuracy) and decreases memorization. Weight decay of 0.3 gives near optimal trade-offs. Further increasing wd to 1.0 results in a drastic decrease in model utility, and thus we do not include the results. Increasing the masking ratio from 0 to 0.5 significantly reduces the memorization but at the cost of model utility. While the optimal value of mr would depend on the application and how much tolerance on the model utility loss is acceptable, we find that $mr = 0.3$ achieves a significant reduction in memorization while only moderately impacting the zero-shot accuracy, as shown in Figure 10. Any further increase in mr beyond 0.5 would greatly sacrifice the model utility and thus is not recommended.

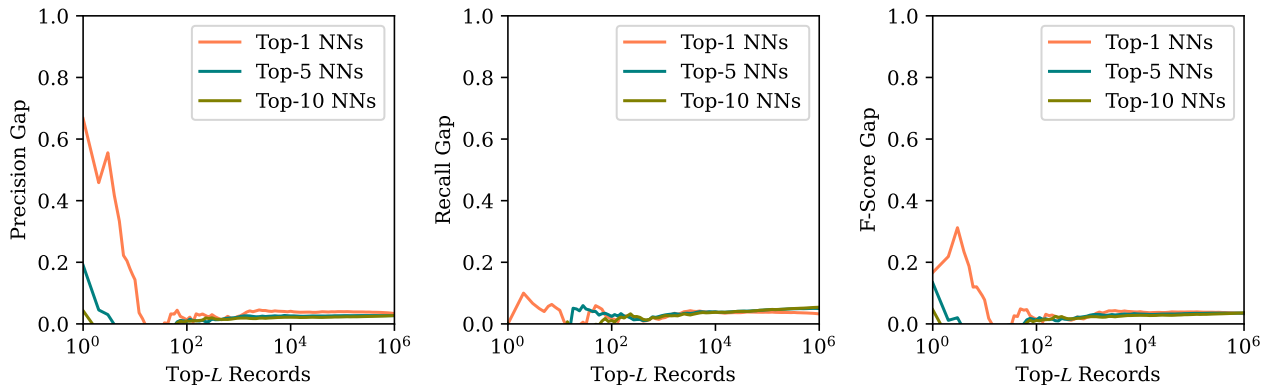


Figure 8: Memorization gap between target and reference models when predicting top-10 objects for different top- L records. Records are sorted w.r.t. the embedding distance. Models are trained on disjoint 10M subsets of filtered LAION data set for 200 epochs and LAION-50M public set is used for the KNN test.

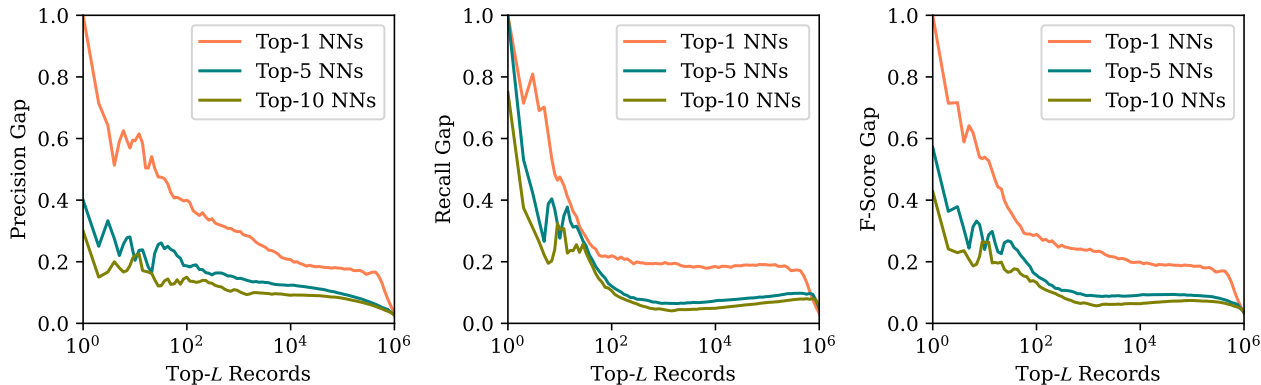


Figure 9: Memorization gap between target and reference models when predicting top-10 objects for different top- L records. Records are sorted w.r.t. the decreasing number of correct object predictions for target model. Models are trained on disjoint 10M subsets of filtered LAION data set for 200 epochs and LAION-50M public set is used for the KNN test.

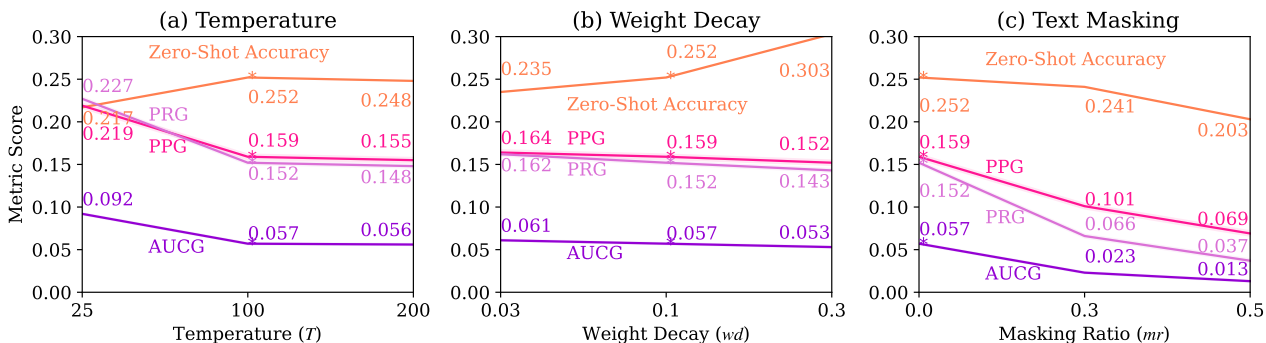


Figure 10: Effect of parameter tuning on ViT-B-32 CLIP models trained on 10M subset of filtered LAION for 200 epochs. Memorization evaluation is done using LAION-50M as public set. Default setting is highlighted with asterisk. For the memorization metrics, we report the $mean \pm std$ values ($std \leq 0.003$) over 100 repetitions of randomly sampling 10% of records with replacement.



Figure 11: Additional examples showing déjà vu memorization. Target images are from COCO training set and the public images are from ImageNet data set. The objects annotated in orange are true positives, i.e., the ones present in the target image, and the objects annotated in blue are false positives.